Sensors & Transducers, Vol. 197, Issue 2, February 2016, pp. 58-66

Sensors & Transducers

http://www.sensorsportal.com

SmartLab Magnetic: A Modern Paradigm for Student Laboratories

Javier MARTINEZ-ROMAN, Angel SAPENA-BAÑO
Manuel PINEDA-SANCHEZ and Ruben PUCHE-PANADERO
Universitat Politècnica de Valencia, C.Vera s/n, 46022 Valencia, Spain
Tel.: 34-963877592, fax: 43-963877599
E-mail: jmroman@die.upv.es

Received: 5 February 2016 /Accepted: 27 February 2015 /Published: 29 February 2016

Abstract: Undergraduate laboratories should provide means to help the student visualize often complex concepts, to achieve a more lasting understanding and, thus, a more significant learning of the ideas presented in the lectures. However, the laboratories often require students to struggle with complex instrumentation operation and tedious data collection and processing that affect negatively their motivation and distract off the learning objectives. This paper introduces through a specific implementation a recent paradigm for student laboratories, designated as SmartLabs, as an effort to help overcome these drawbacks. SmartLabs Magnetic is a combination of existing magnetic circuits test equipment plus a versatile sensors set combined with a standard and affordable data acquisition card and a portable device App. SmartLab Magnetic collects data during magnetic circuits laboratory tests, processes this data to provide results more easily related to the basic concepts being tested and manages the data into reports that can be sent to the student e-mail account within the App. Students' opinions of the relevance, usefulness, and motivational effect of the new SmartLab Magnetic were very positive.

Keywords: Undergraduate laboratories, Data acquisition and processing, Magnetic circuits, Magnetic saturation, Magnetic losses, Reluctance.

1. Introduction

Undergraduate laboratories should provide means to help the student visualize often complex concepts, to achieve a more lasting understanding and, thus, a more significant learning of the ideas presented in the lectures. As an example, magnetic circuits are often an introductory aspect of under-graduate electrical machines courses [1-5]. Basic learning objectives in these courses are that students should be able to understand how the magnetic circuits work, and calculate their main relationships, such as those between core dimensions, core flux and exciting current. Student must be aware that some lamination properties (such as permeability and total specific losses) are directly related to the electrical machine's fundamental performance figures such as efficiency, the no-load current, or the power factor. Traditionally, students have been able, to a very limited extent, to check these facts experimentally with no-load tests at different voltages on typical electrical machines, like transformers and induction machines, using simple measuring equipment like voltmeters and ammeters or more complex like oscilloscopes.

The student often faces challenges when integrating laboratory and lectures learning. With respect to electromagnetism and electrical machines these challenges are mainly related to the use of

abstract concepts that are hard to visualize [6-7], and to the lack of appropriate and easy to use measurement equipment and test rigs. In the case of electromagnetism, these difficulties are sometimes aggravated by the use of a mathematical approach when actually the students need to visualize the concepts to fully understand them. In recent decades the use of simulations to help visualize those abstract concepts [7], and to simulate the actual electrical machine performance during tests [8-11] has sometimes been adopted but then new drawbacks arise. The SmartLab approach, proposed here, blends the test of actual machines of classical experiments with the enhanced data processing and visualization offered by simulations, in an attempt to profit from their advantages while avoiding their weaknesses.

SmartLabs (SLs) complement the existing equipment under test of classical experiments with a sensors set, a Digital Acquisition (DAQ) board and a portable device App providing DAQ control, acquired data manipulation and handling, and the user interface. Similar approaches based on personal computers, often designated as Virtual Instruments (VI) using the widespread manufacturer terminology, has been shown to have many advantages over traditional instruments. Reference [12], as early as 1984, showed the suitability of VIs to help students get a 'real-time' handle on some electrical machine concepts. In [13], efficient data collection and manipulation by means of VIs is shown to help maintain student interest and reduce the time required to perform and evaluate experiments; similar advantages were reported in [14]. VIs' ability to provide user-friendly interaction with the experiment is also underlined in [15]. The modular and reusable nature of Vis, and therefore their suitability for integration into cost-effective systems is underlined in [16]. Additional benefits from having students collaborate in VI development is that these then reflect student interests and needs, as described, along with already mentioned advantages, in [17]. With respect to magnetic materials properties, some advantages are also cited in [18-19] and [20].

SmartLab Magnetic (SLM) was the first SmartLab developed by the Installations, Systems and Electrical Equipment (iSEE) group (within the Institute for Energy Engineering of Universitat Politècnica de València) out of five already deployed and several more under development. SLM is based on the original magnetic circuits lab, which focused on changes in magnetic circuit structure and their effect on winding inductance and no-load current based on rms voltage and current measurements.

This paper first briefly introduces, in Section 2, the main relationships between winding voltage, core flux, core dimensions and materials and exciting current in transformer-core type magnetic circuits, how these influence key electrical machine performance figures and how they relate to various aspects of the no-load current of a transformer. Section 3 describes the equipment under test, and the sensors set and DAQ card. Section 4 deals with the Android App User Interface (UI) design and the required data processing and handling that enhances visual recognition of the main relationships in Section 2 while providing a friendly user experience. Section 5 describes the tests to be performed and the data to be collected to arrive at the main results directly related to the lab's learning objectives. Finally, the student opinion on the relevance, usefulness and motivational effect of the laboratory is detailed in Section 6. The main conclusions of are presented in Section 7.

2. Introduction to Transformer-Core Type Magnetic Circuits

Transformer-core type magnetic circuits are characterized by a set of stretches linked in series (sometimes, as a result of symmetry two identical sets are arranged in parallel, as in the shell type core) along which the magnetic flux is quite approximately constant. As a result of this, the magnetic behavior of each stretch can be depicted by its reluctance:

$$F = \Re\Phi \;;\; \Re = \frac{l}{\mu S} \tag{1}$$

For the whole magnetic circuit, as a series combination of several tracts or limbs, when excited by a single winding with N turns, results:

$$N \cdot I = mmf = \sum \Re_{tract}\Phi = \Re_{core}\Phi \tag{2}$$

Thus, longer magnetic circuit tracts or smaller available core cross-section result on a higher reluctance and a higher no load current for the same core flux. Also, as the core iron saturates its average permeability decreases and the higher reluctance means again more exciting current is needed.

The transformer being at no load, the winding sinusoidal voltage is almost equal to the induced electromotive force (emf) that, in turn, requires a sinusoidal core flux that must lag the winding voltage by ¼ period:

$$\begin{aligned} & u(t) = \sqrt{2}U\cos(\omega t) = N\frac{d\Phi_{core}}{dt} \Rightarrow \\ & \Rightarrow \Phi_{core} = \frac{\sqrt{2}U}{N\omega}\cos(\omega t - \pi/2) \end{aligned} \tag{3}$$

The winding no-load current, necessary to provide the magnetic circuit magnetomotive force (mmf) and to support its losses, can then be split into its magnetizing and iron-loss components. The magnetizing current is in phase with flux pulsation but, due to core saturation, exhibits obvious peaks (in phase with core flux peaks which, in turn, coincide with the zero voltage instant due to the ¼ period lag) that results in a bell-shaped waveform. The iron-loss current is in phase with the winding voltage and, therefore, leads the magnetizing current by a ¼ period. The result of this phase shift between the two no-load

current components appears as a left-peak-right asymmetry of the no-load current semi-periods (see for example [4], pp. 81-84 or [5], chapter 2.4.2.3).

From an electrical engineer's point of view, the core's magnetic materials main properties are the permeability and specific losses, because they are directly related to fundamental performance figures of the electrical machine. The iron core mmf accounts for between 30 % (in rotating electrical machines) to 90 % (in transformers) of the total required mmf, the remaining percentage being due to airgaps. In turn, the total mmf is directly related to the machine's no-load current and, through that, to its power factor and to the reactive power consumption. The ES specific losses are directly related to the core losses, amounting to about one third of the machine's total losses. The remaining losses are mainly Joule effect losses in the windings and friction losses in rotating machines. ES specific losses are closely proportional to core's induction squared and, therefore, for the same core flux, the smaller the available core cross-section the higher the specific losses.

3. Test Equipment

The test equipment that integrates the SLM has been derived from the original laboratory equipment used with classic instrumentation. It included a variable autotransformer to provide adjustable voltage at constant mains frequency, a three phase three leg transformer (220/380 V, 2 kVA), one voltmeter and one ammeter. The classic instrumentation was the only element enhanced for the SLM.

3.1. Magnetic Circuit Configurations

A three phase transformer is used to test different magnetic circuits with varying configurations (see Fig. 1 to Fig. 4) depending on the winding being fed or connected and thus give the student the opportunity to correlate changes in magnetic circuit configuration with the observed changes in winding inductance and overall magnetic circuit reluctance. Four tests where thus devised: Series-parallel I, Series-parallel II, Series and Open.

In the Series-parallel I configuration (Fig. 1) only the primary winding on the left leg is fed, at its rated voltage, keeping all other windings open. Thus, the flux required in the left leg goes through the left yoke to the junction between the central leg and the right yoke and leg, where it splits, mostly going through the shorter central limb.

In the Series-parallel II (Fig. 2) configuration only the primary winding on the central leg is fed, at its rated voltage, keeping all other windings open. Thus, the flux required in the central leg goes to the junction between the left and right legs where it splits approximately halves. In this configuration magnetic flux lines are, in average, shorter, and the full magnetic flux is confined in a single limb for a shorter tract. These two configuration changes result in a lower magnetic circuit reluctance.

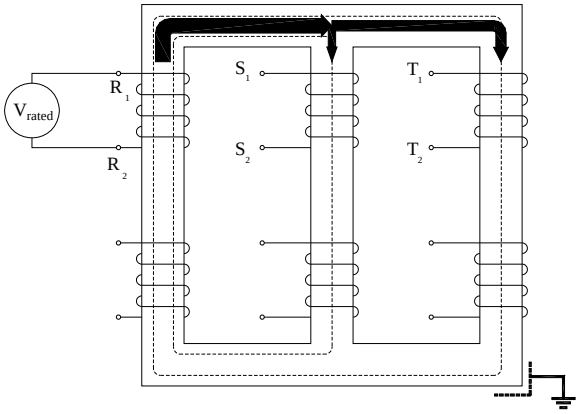

Fig. 1. Series-Parallel I magnetic circuit.

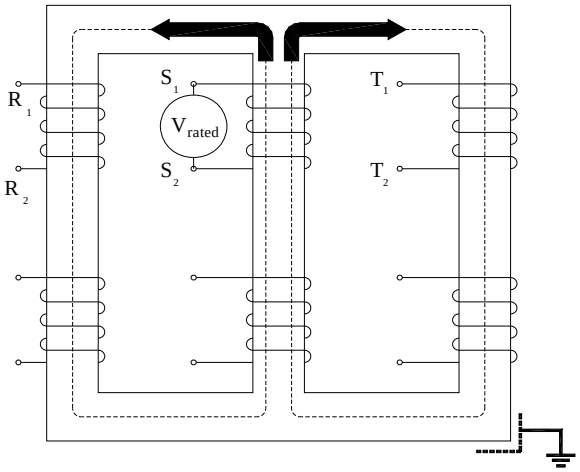

Fig. 2. Series-Parallel II Magnetic Circuit.

In the Series configuration (Fig. 3), again, only the primary winding on the central leg is fed, at its rated voltage, keeping all other windings open but the secondary winding on left leg, which is short-circuited. Thus, no voltage means almost no winding induced emf nor flux in the left leg and the flux required in the central leg goes to right leg almost fully. Now the magnetic flux lines are more or less the same length as those in Series-Parallel II magnetic circuit but the available iron cross-section has been halved along most of the magnetic circuit. Thus the magnetic circuit reluctance clearly increases.

Finally, in the Open Circuit configuration (Fig. 4), again, only the primary winding on the central leg is fed, at a fraction of its rated voltage, keeping all other windings open but the secondary winding on both the left and right legs, which are now short-circuited. Thus the flux required in the central leg must close through a mostly non-ferromagnetic path surrounding the winding. The deepest change in the magnetic circuit is

the change of ferromagnetic to non-ferromagnetic material on most of its length and the magnetic circuit reluctance drastically increases.

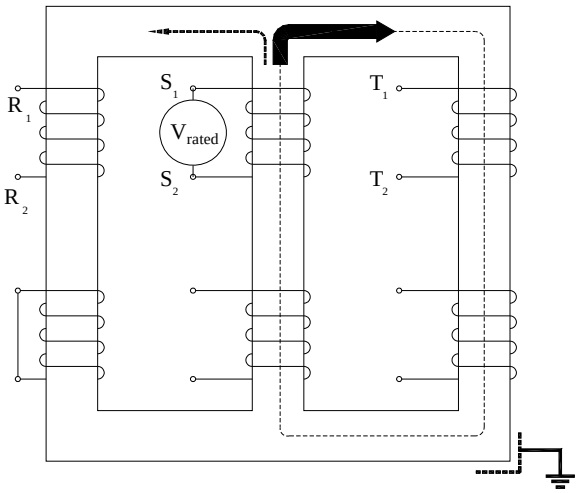

Fig. 3. Series Magnetic Circuit.

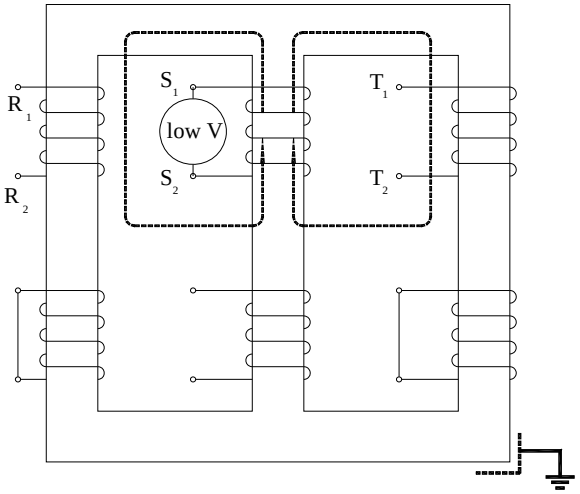

Fig. 4. Open Magnetic Circuit.

3.2. SLM Enhanced Instrumentation

The classic volt- and ammeter provided very interesting feedback on the magnetic circuit performance but that information can be clearly improved to enhance the student recognition of the basic phenomena taking place during the tests. Thus, instead of working with rms voltage and current sensors it was decided to substitute them by wide bandwidth voltage sensors and, additionally, to simplify the measurements, to include direct voltage measurement or the three primary windings.

The voltage sensor selected is a differential grounded voltage divider, which provides easily adjustable attenuation, very good bandwidth including DC voltages if required, and low common voltage suitable for a DAQ card differential analog input. Isolation is not required due to the use of low voltage mains and to the grounded divider configuration. The current sensor selected is a closed loop, compact, multirange Hall Effect current transducer (LEM LTS 6 NP) which provides very good bandwidth, easy integration, 3 kV voltage isolation, and low common mode output while requiring single unipolar voltage supply.

Finally, as can be appreciated from Fig. 1 to Fig. 4, the flux distribution in the three core legs changes considerably for the four configurations being tested. This flux distribution can be directly correlated to the respectively fed/induced voltage in each of the primary windings, which makes it quite interesting to provide the user with voltage readings simultaneously for all primary windings.

The sensors described are complemented (Fig. 5) with a Measurement Computing BTH-1208LS DAQ card. This card is selected because it is one of the very few available with built in Bluetooth communication and Android support, thus enabling a direct integration with Android Apps and, especially, a simple and easily configurable link between the DAQ card and the mobile device. The BTH-1208LS has 4/8 differential/single-ended analog inputs with a maximum shared sample rate of 47 kS/s, apart from two analog outputs, 8 digital input/outputs and a high-speed counter input, which can be used in different applications (e.g., reactive power compensation, discharge lamp lightning control or frequency converter drive operation, no described here [21-24]). The maximum sampling frequency of 47 kS/s is quite enough for this application as it requires four channels, one current and three voltages, with a suitable resolution to depict up to harmonic 19 at most. Thus an individual sampling frequency resulting in 5 samples per period for the highest harmonic, about 5 kS/s, is quite enough, which results in an aggregated sampling frequency of 25 kS/s, clearly below the DAQ card maximum sampling frequency.

The DAQ and sensors board are placed inside a rugged plastic case together with a short-circuit protection, the required power supply and the suitable mains and measurement connections (Fig. 6).

4. SLM App User Interface Design

The SLM App UI design is based on these main objectives:

a) Provide a clear reading of the test rms voltages and currents,
b) Complement those readings with the fed voltage and current waveforms and
c) Also with the comprehensive magnetic cycle of the magnetic circuit,
d) Facilitate data gathering with in-built report generation and delivery.

To this end, the user interface is divided into three main areas: readings, graphs and App menu (Fig. 7).

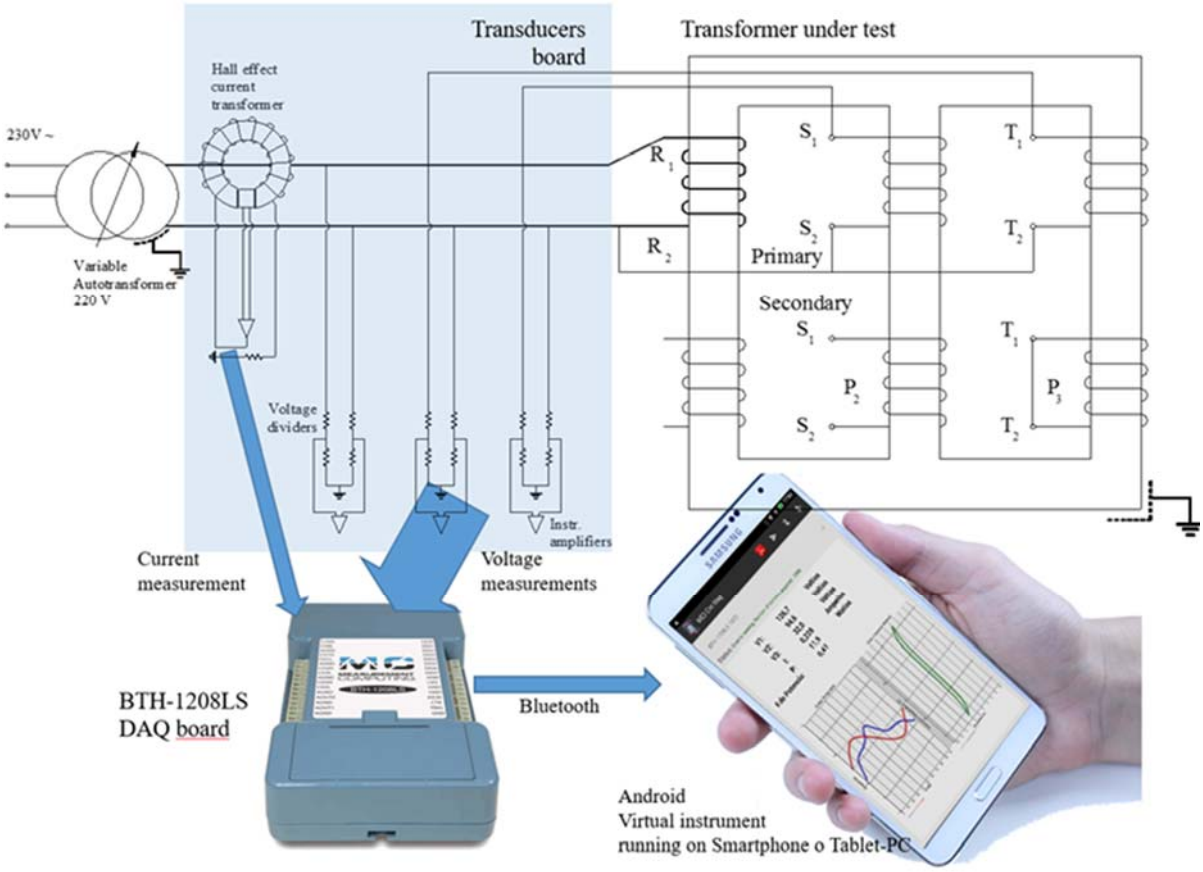

Fig. 5. SLM Instrumentation: Voltage and current sensors, DAQ Card and Virtual Instrument Android App.

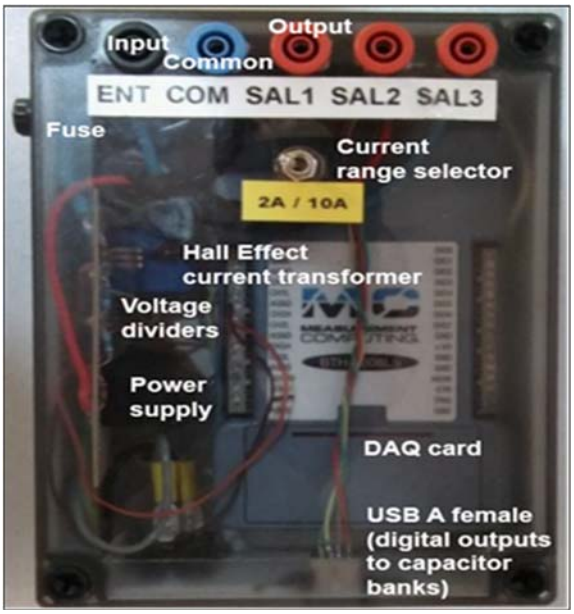

Fig. 6. DAQ and sensors casing with external connections.

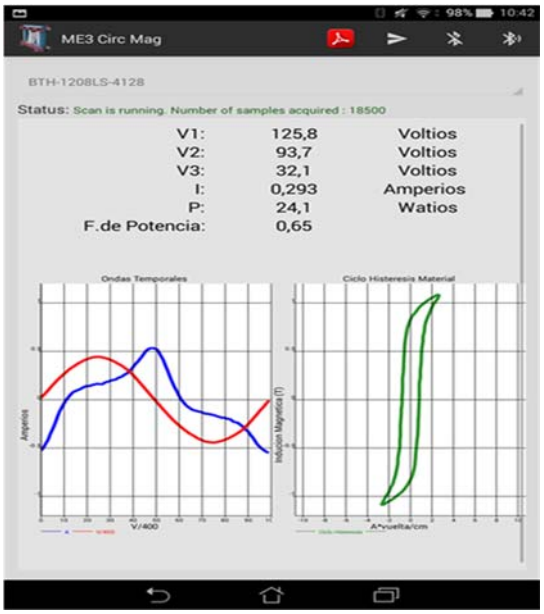

Fig. 7. SLM App user interface main areas: readings, graphs and App menu.

The readings area, apart from the rms voltages (three, one in each of the three primary windings) and current, includes also the power consumption and the power factor to provide the student notions on *real* magnetic circuits with actual iron losses and their importance on electrical machines operation and performance. The rms values are calculated as the square root of the current and voltage sample's squares average. The electric power is calculated as the average current and voltage sample's products and, with the apparent power, V·I, is used to calculate de power factor.

The graphs area is shared between the current and voltage time-waveforms and the comprehensive magnetic cycle. The voltage and current time waveforms are a direct trace of the sampled voltage and current during one mains period. The voltage and current arrays are first rearranged to force a start with a voltage positive zero crossing. This simple operation helps readability as it behaves like a mains trigger locking the time-waveforms in the horizontal axis. The learning objectives especially related with the time-waveforms are the following ones:

a) Mains connected electrical machines, and, specifically, transformers, operate with very closely sinusoidal voltage and flux, no matter how saturated the core is,

b) Core saturation results in no-load current deformation with asymmetrical bell shaped waveforms that account for saturation and iron core losses, and,

c) Current waveform asymmetry swells the left side of each half period around the current maximum, resulting in a leading current component, the iron loss current.

The comprehensive magnetic cycle is traced as a xy-curve of core average induction vs. core average field strength. The average core induction is calculated from the core flux using the known core dimensions, while the core flux is obtained through a quarter period shift of the winding voltage samples array and using known winding turns and mains frequency. On the other hand, the core's average field strength is calculated from the winding current samples array times the winding turns (mmf) and divided by the core mid-line length. The learning objectives especially related with the comprehensive magnetic cycle are the following ones:

a) Changes in the magnetic circuit reluctance result in inversely related changes on the magnetic cycle average slope, and,

b) Changes in the magnetic circuit losses result in direct changes on the magnetic cycle enclosed area.

The great advantage, however, in including the comprehensive magnetic cycle graph is to provide the student a lasting image that can be easily correlated with basic concepts of ferromagnetic materials. This image has the additional benefit of helping the user correlate simple changes in the magnetic circuit with directly recognizable features of the graph: for example, when the average flux lines length decreases from series-parallel I to series-parallel II, the user can directly associate that change to a slope increase in the magnetic cycle slope.

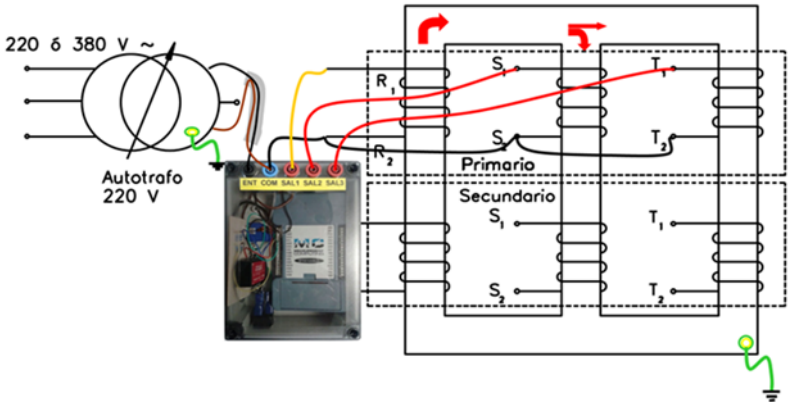

Fig. 8. Circuit Schematic for series-parallel I magnetic circuit in student laboratory notes.

Finally, with regard to the App menu, it includes buttons to generate a report in PDF format which includes both the readings and the graphs for the actual test being performed and also to send by email the reports generated during the laboratory session [25]. This actions are complemented with the Bluetooth connection and disconnection buttons required to establish or break the link with the DAQ card. The fact that the user does just need to press a button to generate a test report with the actual conditions and graphs and another to receive in his/her email inbox all the reports for the session experiments means that a significant amount of the session allotted time which was traditionally dedicated to data collection and processing can be now devoted to analyze test results, elaborate correlations, combine observations and prepare conclusions. This, by avoiding tedious tasks, adds also to the student motivation.

The SLM App is available for download in Google Play [26]. From there the students can download and install it in their Android mobile devices. One paired with the DAQ card by Bluetooth, they can use them to perform the measurements instead of with the tablet-PCs available in the Laboratory.

6. SLM Tests Guide and Main Results

The student laboratory work is organized in four consecutive tests that help him correlate different changes in the configuration of the magnetic circuit with the observed changes in the measured voltages and currents and, especially, with the shape (slope and area) of the comprehensive magnetic cycle. The four test to be performed are directly related with the

four magnetic circuit configurations described in Section 3.1.

The student work is guided with the help of easy to follow schematics (Fig. 9) of the electric circuits required in each test and a check list procedure to perform them. In these schematics, a simple color code is used to help distinguish the different connections and the changes to be made from one experiment to the next. Attention is also drawn to safety measures to avoid voltages or currents above those rated for the equipment under test or for the transducers.

Fig. 9. SLM page on Play Store (Google).

The laboratory notes draw the attention to the changes to be observed between consecutive experiments. Thus, from the series-parallel I (Fig. 7) to the series-parallel II magnetic circuits (Fig. 10) the user can notice a reduction of the no load current and also of the magnetic losses, along with an increase in the comprehensive magnetic cycle average slope. These observations can be readily be associated to the reduction in average length of the magnetic flux lines together with an increase in the average available iron cross-section.

Then, from the series-parallel II (Fig. 10) to the series magnetic circuit (Fig. 11) the user can notice an increase of the no load current and also of the magnetic losses, along with a reduction in the comprehensive magnetic cycle average slope. These observations can be readily be associated to the reduction in the average available iron cross-section.

Finally, from the series magnetic circuit to the open magnetic circuit the user can realize that current consumption is quite higher, even for a drastically reduced winding voltage, and a very reduced slope in the comprehensive magnetic cycle that has now a very small enclosed area (Fig. 11). These observations can be immediately connected to the high reluctance magnetic circuit in which magnetic flux lines have been drawn out of the iron core.

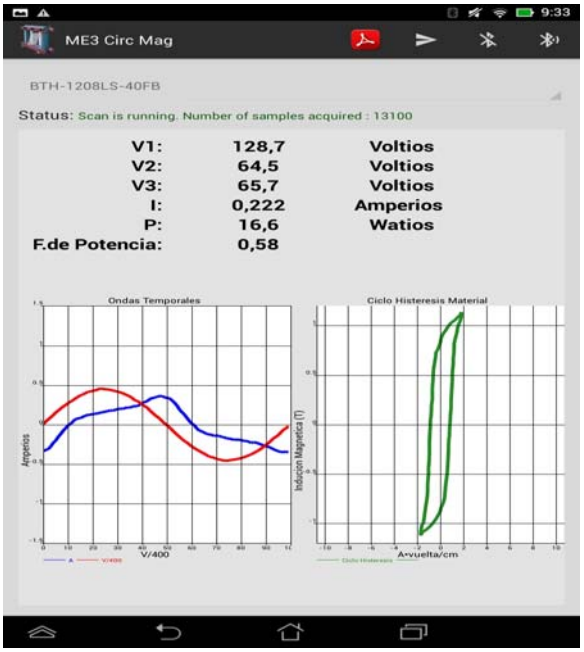

Fig. 10. Series-parallel II magnetic circuit test results.

7. Evaluation

SLM was used during the Spring 2014 and 2015 semesters by UPV's GITI and GIE students, and had previously been tested with the students of earlier degree programs. SLM's effectiveness was assessed by means of a student survey administered after the laboratory.

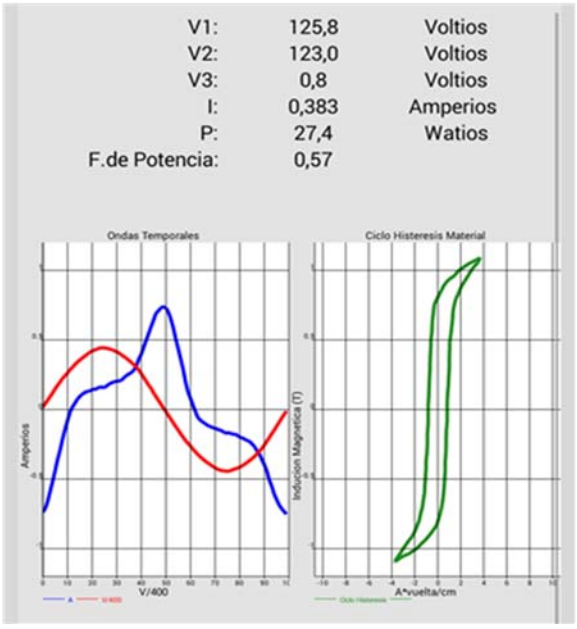

Fig. 11. Series magnetic circuit test results.

This assessment was conducted only on some of the laboratory sessions, because of the significant time required to sit the regular exams and then complete the survey and in total 127 students answered the survey.

The student satisfaction survey had five statements with a five-point scale, from 1 (completely agree) to 5 (completely disagree):

S1. This laboratory was useful for your education on electrical machines

S2. This laboratory helped you to understand concepts and enabled you to apply them in the topic being studied

S3. This laboratory increased your motivation towards learning electrical machines

S4. This laboratory provided you with useful experience that might be of service in your future job

S5. The educational materials used in this laboratory were adequate for the tasks to be performed.

The results of this survey, summarized in Fig. 13, show a good level of student satisfaction with the laboratory, with responses falling mainly between "completely agree" and "agree". The best scores were for statements S1 (usefulness), S2 (aid to understanding and applicability) and S5 (adequacy of the materials), all with over 70 % of responses being between "completely agree" and "agree".

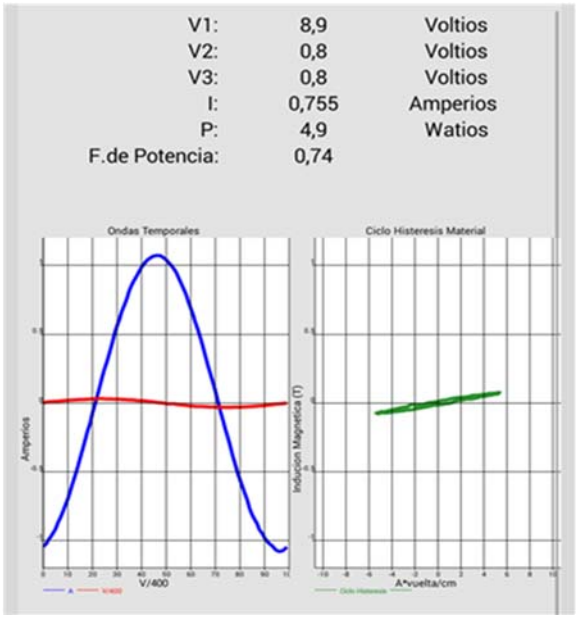

Fig. 12. Open magnetic circuit test results.

8. Conclusions

Blending modern technologies like DAQ boards and mobile devices Apps with traditional electrical machines laboratory equipment has been shown to have many advantages.

Modern test equipment and a set of laboratory tests on electrical machines' magnetic circuits configuration were developed to exploit these advantages, with the aim of helping students visualize complex concepts related with them, achieve a more lasting understanding and, thus, a more significant learning of the ideas presented in the magnetic circuit lectures.

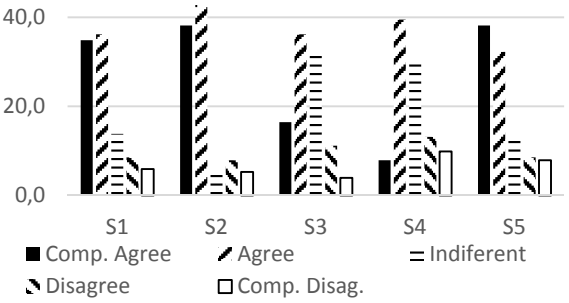

Fig. 13. Student satisfaction survey responses to statements S1 to S5.

The test equipment captures voltage and current waveforms during the no-load operation of a transformer fed in different ways to set-up four varied magnetic circuit configurations. It then processes and presents the actual measured voltage and current waveforms together with the calculated core flux waveform, rms values, power losses and the core magnetic cycle on the screen of an Android mobile device. In this way, through a guided set of tests, the students can directly link the main properties of the magnetic circuit (average flux lines length, iron cross-section, permeability and specific losses) with basic operation parameters of the transformer (mainly the no-load current and core losses) and, specially, with the time waveforms and the magnetic cycle peculiarities.

The combination of the guided exercises with the SLM test equipment developed results in high levels of student satisfaction with the laboratory work, and thus, improved student motivation showing that the main objectives set during the laboratory design were achieved.

References

[1]. S. A. Nasar, L. E. Unnewehr, Electromechanics and electric machines, 2nd ed., *Wiley*, New York, 1983.

[2]. M. G. Say, Alternating current machines, 5th ed., *John Wiley & Sons*, 1983.

[3]. A. E. Fitzgerald, C. Kingsley, S. D. Umans, Electric Machinery, 6th ed., *McGraw-Hill International Edition*, New York, 2003.

[4]. S. J. Chapman, Electric Machinery Fundamentals, 5th ed., *McGraw-Hill*, 2011.

[5]. L. Serrano-Iribarnegaray, J. Martínez-Román, Máquinas Eléctricas, 3rd ed., *Editorial de la Universitat Politècnica de València*, 2014.

[6]. S. Bentz, Integration of basic electromagnetism and engineering technology, in *Proceedings of the Frontiers in Education Conference*, Vol. 2, November 1995, pp. 4a5.4–4a5.7.

[7]. V. Pulijala, A. Akula, A. Syed, A web-based virtual laboratory for electromagnetic theory, in *Proceedings*

of the IEEE 5th International Conference on Technology for Education (T4E), December 2013, pp. 13-18.
[8]. S. Ayasun, C. Nwankpa, Induction motor tests using Matlab/Simulink and their integration into undergraduate electric machinery courses, *IEEE Transactions on Education*, Vol. 48, Issue 1, Feb. 2005, pp. 37-46.
[9]. A. Bentounsi, H. Djeghloud, H. Benalla, T. Birem, H. Amiar, Computer-aided teaching using matlab/simulink for enhancing an in course with laboratory tests, *IEEE Transactions on Education*, Vol. 54, Issue 3, Aug. 2011, pp. 479-491.
[10]. M. Ojai, J. Fail, M. Kazembe, M. Rezaian, Performance analysis of saturated induction motors by virtual tests, *IEEE Transactions on Education*, Vol. 55, Issue 3, 2012, pp. 370-377.
[11]. A. Seal, K. Gaurav, T. Monger, Virtual laboratory platform for enhancing undergraduate level induction motor course using matlab/simulink, in *Proceedings of the IEEE International Conference on Engineering Education: Innovative Practices and Future Trends (AICERA)*, July 2012, pp. 1-6.
[12]. S. Gruber, A computer-interfaced electrical machines laboratory, *IEEE Transactions on Education*, Vol. 27, Issue 2, 1984, pp. 73-79.
[13]. J. M. Williams, J. L. Cael, N. D. Benavides, J. D. Wooldridge, A. C. Koenig, J. L. Titchener, S. D. Peaker, Versatile hardware and software tools for educating students in power electronics, *IEEE Transactions on Education*, Vol. 47, Issue 4, 2004, pp. 436-445.
[14]. J. M. Jiménez-Martinez, F. Soto, E. d. Jodi, J. A. Villarejo, J. Roca-Dorda, A new approach for teaching power electronics converter experiments, *IEEE Transactions on Education*, Vol. 48, Issue 3, 2005, pp. 513-519.
[15]. F. Sellschopp, L. Arjona, An automated system for frequency response analysis with application to an undergraduate laboratory of electrical machines, *IEEE Transactions on Education*, Vol. 47, Issue 1, 2004, pp. 57-64.
[16]. S. Durovic, Development of a simple interactive laboratory exercise for teaching the principles of velocity and position estimation, *International Journal of Electrical Engineering Education*, Vol. 50, No. 3, 2013, pp. 256-267.
[17]. W. Heath, O. Onel, P. Green, B. Lennox, Z. Gai, Z. He, M. Rodriguez Liñan, Developing a student-focused undergraduate laboratory, *International Journal of Electrical Engineering Education*, Vol. 50, No. 3, 2013, pp. 268-278.
[18]. T. Sloane, Laboratories for an undergraduate course in power electronics, *IEEE Transactions on Education*, Vol. 38, No. 4, Nov. 1995, pp. 365-369.
[19]. J. Van't Hof, J. Bain, R. M. White, J.-G. Zhu, An undergraduate laboratory in magnetic recording fundamentals, *IEEE Transactions on Education*, Vol. 44, Issue 3, Aug. 2001, pp. 224-231.
[20]. J. Martinez-Roman, J. Perez-Cruz, M. Pineda-Sanchez, R. Puche-Panadero, J. Roger-Folch, M. Riera-Guasp, A. Sapena-Bano, Electrical machines laminations magnetic properties: A virtual instrument laboratory, *IEEE Transactions on Education*, Vol. 58, Issue 3, 2015, pp. 159-166.
[21]. J. Martinez-Roman, J. Fernandez-Molina, A. Sapena-Bano, M. Pineda-Sanchez, R. Puche-Panadero, Magnetic materials and magnetic circuits SmartLab, in *Proceedings of the XVII International Symposium on Electromagnetic Fields in Mechatronics, Electrical and Electronic Engineering (ISEF'15)*, 2015.
[22]. J. Martinez Roman, R. Gomis-Cebolla, A. Sapena-Bano, J. Perez-Cruz, Reactive power compensation SmartLab, in *Proceedings of the XVII International Symposium on Electromagnetic Fields in Mechatronics, Electrical and Electronic Engineering (ISEF'15)*, 2015.
[23]. J. Martinez Roman, J. Perez-Cruz, M. Pineda-Sanchez, R. Puche-Panadero, A. Sapena-Bano, Smartlabairgap: Rotating electrical machines airgap field laboratory, in *Proceedings of the XVII International Symposium on Electromagnetic Fields in Mechatronics, Electrical and Electronic Engineering (ISEF'15)*, 2015.
[24]. J. Martinez Roman, J. Bermudez-Campos, A. Sapena-Bano, J. Roger-Folch, M. Riera-Guasp, Pumping station expert and control system on an android virtual instrument, in *Proceedings of the XVII International Symposium on Electromagnetic Fields in Mechatronics, Electrical and Electronic Engineering (ISEF'15)*, 2015.
[25]. iSEE (Instalations Systems and E. E. A. I. UPV, "SmartLab magnetics test reports", 02 2016. [Online]. http://¬personales.upv.es/¬jmroman/¬SLM/¬test_reports.avi
[26]. "Google play store: SmartLab-magnetics", [Online]. https://¬play.google.com/¬store/¬apps/-details?id=com.smartlab.magnetic